The latest version is at http://www.jbc.org/cgi/doi/10.1074/jbc.RA119.006974

Collagenolytic matrix metalloproteinases antagonise proteinase-activated receptor-2 activation, providing insights into extracellular matrix turnover

Adrian M.D. Falconer[1], Chun Ming Chan[1], Joseph Gray[2], Izuru Nagashima[3], Robert A. Holland[4], Hiroki Shimizu[3], Andrew R. Pickford[4], Andrew D. Rowan[1,*], David J. Wilkinson[1,*]

From the [1]Skeletal Research Group, Institute of Genetic Medicine, Newcastle University, Central Parkway, Newcastle-upon-Tyne, NE1 3BZ, UK; [2]Institute of Cell and Molecular Biosciences, Newcastle University, Framlington Place, Newcastle-upon-Tyne, NE2 4HH, UK; [3]Bio-material Engineering Research Group, Bioproduction Research Institute, Department of Life Science and Biotechnology, National Institute of Advanced Industrial Science and Technology (AIST), Sapporo, Hokkaido 062-8517 Japan; [4]Centre for Enzyme Innovation, School of Biological Sciences and Institute of Biological and Biomedical Sciences, University of Portsmouth, King Henry Building, King Henry I Street, Portsmouth, PO1 2DY

Running title: *MMPs antagonise PAR2 signalling*

To whom correspondence should be addressed: David J. Wilkinson, david.wilkinson@newcastle.ac.uk; *Authors share senior authorship

Keywords: Proteinase-Activated Receptor-2 (PAR2), Matrix Metalloproteinase (MMP), cell signaling, proteolysis, chondrocyte, arthritis, extracellular matrix, inflammation, collagenase

ABSTRACT

The collagenase subfamily of matrix metalloproteinases (MMP) have important roles in the remodelling of collagenous matrices. The proteinase-activated receptor (PAR) family have a unique mechanism of activation requiring proteolysis of an extracellular domain forming a *neo*-N terminus which acts as a tethered ligand, a process that has been associated with the development of arthritis. Canonical PAR2 activation typically occurs via a serine proteinase at Arg^{36}-Ser^{37}, but other proteinases can cleave PARs downstream of the tethered ligand and "disarm" the receptor. To identify additional cleavage sites within PAR2, we synthesised a 42-amino acid peptide corresponding to the extracellular region. We observed that all three soluble MMP collagenases - MMP-1, MMP-8, and MMP-13 - cleave PAR2 and discovered a novel cleavage site (Ser^{37}-Leu^{38}). Metalloproteinases from resorbing bovine nasal cartilage and recombinant human collagenases could cleave a quenched fluorescent peptide mimicking the canonical PAR2 activation region, and kinetic constants were determined. In PAR2-overexpressing SW1353 chondrocytes, we demonstrated that the activator peptide SLIGKV-NH_2 induces rapid calcium flux, inflammatory gene expression (including *MMP1* and *MMP13*), and the phosphorylation of extracellular signal–regulated kinase (ERK) and p38 kinase. The corresponding MMP cleavage–derived peptide (LIGKVD-NH_2) exhibited no canonical activation, however we observed phosphorylation of ERK, providing evidence of biased agonism. Importantly, we demonstrated that pre-incubation with active MMP-1 reduced downstream PAR2 activation by a canonical activator, matriptase, but not SLIGKV-NH_2. These results support a role for collagenases as proteinases capable of disarming PAR2, revealing a mechanism which suppresses PAR2-mediated inflammatory responses.

Proteinases are enzymes that effect proteolysis of intact proteins via the hydrolysis of peptide bonds(1) and are essential in a myriad of situations in both health and disease, such as extracellular matrix (ECM) remodelling during development or pathological destruction. In humans, almost two thirds of the proteinases that comprise the degradome(2) exert their activities within the extracellular space making

them prime candidates in events that entail remodelling and/or degradation of the ECM. These can be sub-divided into metallo- and serine proteinases, and in this context these proteinases have until recently been viewed as mediating the proteolytic degradation of ECM components as occurs for example in tumour invasion or arthritis. However, it is now clear that proteinases also perform precise and specific functions in both homeostasis and disease. The cleavage of triple helical collagens such as type II collagen (the major structural component present in cartilage) by the soluble collagenase subset of matrix metalloproteinases (MMP-1, MMP-8 and MMP-13) represents an example of highly specific proteolysis whereby only a single peptide bond is cleavable under normal physiological conditions(3). This initial cleavage then leads to collagen denaturation, concomitant with increased susceptibility to other less specific proteinases and disassembly of the collagen network which is a requirement as cartilage is remodelled into bone during development, but also occurs during cartilage breakdown in degenerative scenarios such as rheumatoid arthritis (RA) and osteoarthritis (OA).

Proteinase activated receptors (PARs) represent one mechanism by which proteinases can delicately regulate cellular responses and are likely to be involved in many disease processes. The importance of PAR2 in the pathogenesis of both inflammatory arthritis and OA has recently emerged, and PAR2 deficiency provides protection in experimental arthritis models(4–9). We have demonstrated that an activator of PAR2, matriptase, induces cartilage destruction in a PAR2- and metalloproteinase-dependent manner(10, 11) and that a related serine proteinase, hepsin, can also activate PAR2 albeit in a markedly less efficient manner(12). Indeed, in complex disease environments (such as arthritis) multiple proteinases could be present to act on PAR2 making our understanding of how PAR2 is activated and regulated important (reviewed in (13)).

PAR2 exhibits receptor plasticity with biased signalling: different proteinases eliciting different downstream responses following cleavage of the extracellular domain which may be of particular importance in modulating inflammatory responses (see (14, 15)). Here, we investigated the effect of collagenolytic MMPs, known to be expressed during ECM remodelling events(16), on PAR2. We identified novel cleavages by MMP-1, -8 and -13 and a primary cleavage site common to all was identified. Collagenase cleavage resulted in antagonism of PAR2 activation, suggesting an important negative feedback mechanism whereby canonical PAR2 activation induces MMP expression whilst MMP activity can subsequently antagonise PAR2.

RESULTS

MMP Collagenases cleave the PAR2 extracellular domain — To determine which collagenolytic MMPs can cleave the extracellular PAR2 sequence, we synthesised a 42-amino acid peptide, corresponding to the N-terminal extracellular region of PAR2 ($PAR2^{31-72}$ peptide) where previous PAR2 cleavage sites have been identified(17–19) (Fig. 1A). After confirming the peptide was cleaved by known PAR2-cleaving proteinases (Fig. 1B) the peptide was incubated with APMA-activated MMP-1, MMP-8 and MMP-13. Silver-stained SDS-PAGE gels of the digested products demonstrated that all three collagenases were capable of cleaving this sequence in a dose-dependent manner (Fig. 1C). Cleavage was subsequently confirmed by reverse phase HPLC (Fig. 2A-C), and peaks were collected and subjected to electrospray MS. Exact mass identifications revealed cleavage sites for each collagenase (Fig. 2D), but interestingly, time course experiments identified a primary cleavage common to all, following Ser^{37} (Fig. 3). This novel site is adjacent to the canonical cleavage site described for trypsin-like serine proteinases, Arg^{36}.

Collagenases cleave a PAR2 synthetic peptide substrate — To further explore and determine kinetic constants for collagenase cleavage of PAR2, a quenched fluorescent peptide mimic of PAR2 was employed (2-Abz-SKGRSLIG-Y(NO_2)). To demonstrate cleavage by native MMPs, the peptide was incubated with conditioned medium from 14-day IL-1+OSM-stimulated bovine nasal cartilage, a well-established model of proteinase-driven cartilage breakdown(10, 20, 21). Cleavage was observed; however, this was completely abolished by the addition of the MMP inhibitor GM6001, but not by serine or cysteine proteinase inhibition (Fig. 4A). Subsequently, recombinant APMA-activated MMP-1, -8 and -13 were shown to cleave the peptide,

with the effect dependent on active site accessibility (Fig. 4B). Velocity was calculated from progress curves at variable concentrations of substrate and the resultant plots are consistent with each collagenase exhibiting Michaelis-Menten kinetics (Fig. 4C). APMA-activated MMP-1, MMP-8 and MMP-13 exhibited similar K_M values for this substrate 36-53 μM, which are similar to that of matriptase (46.6 μM). MMP-13 exhibited the highest turnover number (k_{cat}) of all three collagenases, and therefore the highest catalytic efficiency (k_{cat}/K_M) although this was markedly lower than that of matriptase (Fig. 4D).

Canonical PAR2 activation induces collagenolytic MMP expression — To generate a model of chondrocytes expressing higher levels of PAR2 (as is the case in OA(22, 23)), we overexpressed PAR2 using a lentivirus transduction system. SW1353 cells transduced with a PAR2-expressing lentivirus (hereafter, SW1353-PAR2; dependency of PAR2 expression validated in Fig. S1) were stimulated with the PAR2 activator peptide, SLIGKV-NH_2, which resulted in calcium mobilisation (Fig. 5A). Furthermore, stimulation for varying durations resulted in *ATF3*, *MMP1* and *MMP13* gene expression (Fig. 5B,C). ATF3 is a transcription factor we recently identified as regulating *MMP13* expression following cytokine stimulation(24). Secreted MMP-1 and MMP-13 were subsequently detected in the culture medium 48 hours post-stimulation (Fig. 5D).

The N-terminus generated by collagenase cleavage does not activate canonical PAR2 signalling — Due to the proximity of the primary collagenase cleavage site to the canonical PAR2 activation sequence, the effect of the resultant neo-N-terminus on PAR2 activation was investigated by synthesising a peptide corresponding to the putative tethered ligand: LIGKVD-NH_2 (see Fig. 2D). SW1353-PAR2 cells stimulated with LIGKVD-NH_2, or the control reverse peptide (DVKGIL-NH_2) exhibited no calcium mobilisation (Fig. 6A) nor the expression of *ATF3* or *MMP1* (Fig. 6B).

The collagenase derived PAR2 peptide LIGKVD-NH_2 induces biased Mitogen-activated protein kinase (MAPK) phosphorylation — MAPK phosphorylation is a well characterised downstream output of canonical PAR2 activation(25–27). Indeed, herein we confirm that SLIGKV-NH_2 (Fig. 6C) induces phosphorylation of ERK and p38 at early timepoints. Intriguingly, LIGKVD-NH_2 induced ERK but not p38 phosphorylation (Fig. 6D), whilst the control reverse peptide did not markedly induce either MAPK (Fig. 6E).

Collagenase cleavage antagonises PAR2 — To determine the effect of collagenase cleavage on the potential for PAR2 to be subsequently activated by canonical PAR2 activators, we performed pre-incubation experiments. When recombinant active MMP-1 was pre-incubated with SW1353-PAR2 cells, matriptase-induced PAR2 activation was abrogated, but importantly, activation by SLIGKV-NH_2 was not (Fig. 7A). There was no evidence of *ATF3* induction by MMP1 on either SW1353 control cells or SW1353-PAR2 cells (Fig. 7B). SW1353-PAR2 cells pre-incubated with LIGKVD-NH_2 markedly reduced the capacity for canonical activation by the SLIGKV-NH_2 (Fig. 7C), whereas cells pre-incubated with the control reverse peptide did not (Fig. 7D).

DISCUSSION

It is becoming increasingly clear that proteolysis not only mediates catabolic events but can also act to precisely regulate cellular processes. One such example, the PARs, represent a way in which controlled cleavage of a substrate by different proteinases leads to different downstream events and outcomes. In this study, we outline such regulation of PAR2 by a family of proteinases that, to our knowledge, have not been investigated before in this context. We demonstrated that the collagenases MMP-1, -8 and -13 can cleave the PAR2 extracellular region, with MMP-1 yielding a single product resulting from cleavage at Ser^{37}-Leu^{38} with an additional cleavage at Val^{68}-Leu^{69} observed following MMP-8 and -13 incubations. These cleavage sites are in agreement with the described substrate specificities of the collagenases which show a preference for a hydrophobic residue in the P1' position, a basic or hydrophobic amino acid in the P2' position, and a small amino acid in the P3' position(28–30). Thus, the Ser^{37}-Leu^{38} site fits this preference with leucine, isoleucine and glycine in P1' - P3', respectively; whilst the Val^{68}-Leu^{69} site fits at the P1' and P3' positions (leucine and glycine, respectively). Taken together with time course experiments, it is likely

that Ser^{37}-Leu^{38} is the primary collagenase cleavage site on PAR2. It remains possible, however, that both cleavages could hold functional relevance. For example, following canonical PAR2 activation by mast cell tryptase, signalling has been shown to be attenuated by a secondary downstream cleavage(31).

The kinetic profiles of PAR2 cleavage by the collagenases were explored and compared with matriptase, a potent activator of PAR2(12). Unsurprisingly, all three collagenases were less efficient at cleaving the substrate compared to matriptase (which exhibited similar kinetics to previously published findings(32, 33)), primarily as a result of lower k_{cat} values, with broadly similar K_M values. When considering the enzyme kinetics of the collagenases, it is important to note that APMA-activated proMMPs were utilised, which are not considered to be fully active with 10-25% of maximal activity typically observed when compared to MMP-3 activated proMMP(34); thus, the collagenase kinetics for PAR2 may be underrepresented compared to *in vivo* cleavage. Furthermore, the abundance of MMPs is an important consideration, since tissues undergoing active remodelling, such as during cartilage destruction in arthritis, have high expression levels of MMPs(35–37). Taken together, these data suggest that the collagenases and matriptase can bind PAR2 with broadly similar affinities, but the collagenases are less efficient at turning over the substrate.

Data presented within the present study demonstrate that the addition of active MMP-1 to PAR2-expressing cells, followed by the activation of PAR2 by matriptase exhibit an attenuated level of activation; importantly a result not observed following SLIGKV-NH_2 activation. This observation can be interpreted as cleavage of PAR2 by MMP-1 in a classical disarming mechanism similar to cathepsin G or proteinase 3 disarming of PAR2(17, 38). This would entail the cleavage of PAR2 at Ser^{37}-Leu^{38} thus removing the canonical activation site to leave a disarmed receptor on the surface (as evidenced by full SLIGKV-NH_2 activation).

Cleavage of cell surface receptors by collagenases has previously been described, with both MMP-1(39) and -13(40) having been shown to be able to activate the PAR1 receptor by cleavage at two amino acids upstream, or a single amino acid downstream, of the canonical site, respectively. Furthermore, low levels of trypsin-activated MMP-1 have been previously described to upregulate monocyte chemoattractant protein-1 (MCP-1) in A549 cells (which endogenously express PAR2) however no mechanism nor cleavage site were described(41).

Both PAR2(23) and matriptase(10) are expressed significantly higher in OA chondrocytes than in normal chondrocytes, which may contribute to the elevated levels of MMP-1 and MMP-13 expression observed in the disease(22). We have previously shown matriptase to induce *MMP* expression in explant OA cartilage(10), and herein we show PAR2 activation in chondrocytes leads to the expression and secretion of both these collagenases. To our knowledge, the expression of MMP-1 and MMP-13 in chondrocytes following PAR2 activation is a novel observation, although the addition of SLIGKV-NH_2 to OA cartilage has previously been shown to increase MMP-1 and MMP-13 immunostaining(22). Aside from the collagenases, other MMPs including MMP2(42), MMP3(43) and MMP9(44) have been shown to be induced by PAR2 activation in various cell types.

Biased agonism following activator peptide stimulation of PAR2 has previously been explored. The peptide SLAAAA-NH_2 has been shown to induce ERK1/2 phosphorylation in the absence of calcium mobilisation(45) as observed with LIGKVD-NH_2 in the present study. In rat PAR2, ALIGRL-NH_2 peptide (based on the rat canonical activation sequence, SLIGRL) has been shown to result in detectable canonical PAR2 activation (as measured by calcium mobilisation), with no detectable activation when substituting the P2' leucine for alanine (SAIGRL-NH_2) – identifying a key role for the P2' leucine in canonical activation(46). In the present study, this P2' leucine becomes the P1' leucine and no calcium mobilisation was detected. Furthermore, the presence of a basic amino acid in P5' has been postulated as a requirement for calcium mobilisation(47), which is lost in LIGKVD compared to SLIGKV (underlined). Data presented within the present study suggest competitive binding in the extracellular region of PAR2 between the two similar sequences, SLIGKV and LIGKVD, despite their differing downstream effects. The functional consequences of ERK1/2 phosphorylation induced by the collagenase-derived peptide requires

further investigation, although this does not involve the activation of canonical PAR2 signalling pathways or downstream induced genes such as *ATF3* and *MMP1*.

The data presented herein support a mechanism by which collagenolytic MMPs, the expression of which are induced by canonical PAR2 activation, negatively regulate PAR2 by abrogating its canonical activation (Fig. 8).

EXPERIMENTAL PROCEDURES

Materials — Unless stated otherwise, all chemicals were of the highest purity available and obtained from Sigma Aldrich (Gillingham, UK). All proteins were recombinant human, except cathepsin G and neutrophil elastase which were purified from human sputum (Elastin Products, Owensville, USA). Matriptase(11), hepsin(12) proMMP-1, and proMMP-13(48) were all prepared as previously described. proMMP-8 was obtained from R&D Biosystems (Abingdon, UK). Tissue inhibitor of metalloproteinases-1 (TIMP-1) was a kind gift from Prof Hideaki Nagase (Oxford University, UK). The SLIGKV-NH_2 peptide was purchased from Abcam (Cambridge, UK), (Abz-Ser-Lys-Gly-Arg-Ser-Leu-Ile-Gly-Tyr(NO_2)) substrate was from GL Biochem (Shanghai, China) whilst peptides LIGKVD-NH_2 and DVKGIL-NH_2 were synthesised by Peptide Synthetics (Fareham, UK). MMP inhibitor GM6001 was from Merck Millipore (Watford, UK).

Cell culture — SW1353 chondrosarcoma cells were purchased from American Type Culture Collection (cat. no. HTB-94; Rockville, MD). Cells were cultured at 37°C in DMEM/F-12 medium supplemented with 2 mM L-glutamine, 100 IU ml^{-1} penicillin and 100 µg ml^{-1} streptomycin, and 10% foetal bovine serum (all from Thermo Fisher, Paisley, UK). Cells were starved in serum-free medium for at least 6 hours prior to stimulation.

Lentivirus generation and transduction — The lentiviral expression plasmid pSIEW-hPAR2 was constructed using a BamHI-tagged human PAR2 PCR product generated from the human PAR2 VersaClone cDNA (RDC0166, R&D Biosystems) with primers: For, 5'-AAAA GGATCCGCCACCATGCGGAGCCCCAGC-3' and Rev, 5'-GCGCGGCCGCGGATCCTC AATAGGAGGTCTTAACAGTGGTTGAAC-3' prior to routine sub-cloning into BamHI-digested pHR-SINcPPT-SIEW (a generous gift from Prof. Olaf Heidenreich, Newcastle University, UK).

Lentiviruses were generated in HEK293T cells following transfection with pSIEW-hPAR2, pCMVΔ8.91 and pVSV-G (both supplied by Prof. Heidenreich, Newcastle University, UK) according to standard protocols, and concentrated using the Lenti-X kit (ClonTech, Mountain View, USA).

SW1353 cells at 50% confluency were transduced for 48 hours with lentivirus in serum-containing DMEM-F12 supplemented as above with the addition of 4 µg ml^{-1} polybrene at a 1:200 concentrated virus:medium ratio. Cells were assessed for successful transduction by examining GFP expression using inverted fluorescence microscopy, and then serum-starved for a minimum of 6 hours prior to use.

Peptide Digestion and Visualisation — A 42 amino acid peptide corresponding to amino acids 31–72 of human PAR2 (H_2N-RSSKGRSLIGKVDGTSHVTGKGVTVETVFSV-DEFSASVLTGK-COOH) was synthesised (see Supporting Information), ($PAR2^{31-72}$ peptide). The peptide was incubated at a final concentration of 10 µM with various proteinases at 37°C for varying durations (see Supporting Information for full details of incubation buffers).

For visualisation, samples were resolved on 20% polyacrylamide Tris-Tricine gels(49), which were subsequently fixed for 1 hour in 12% trichloroacetic acid/ 30% methanol followed by silver staining using a Plus One silver staining kit (GE healthcare, Little Chalfont, UK) according to the manufacturer's instructions. Mass Spectrometry (MS) – Analytical reverse phase HPLC (RP-HPLC) and infusion electrospray MS and were performed as previously described(50) with some modifications (see Supporting Information).

Enzyme Kinetics — ProMMPs were activated with 1 mM APMA and then active-site titrated with TIMP-1(51) using Mca-Lys-Pro-Leu-Gly-Leu-Dpa-Ala-Arg-NH_2 (FS-6; Sigma-Aldrich) as substrate. Matriptase was titrated using 4-methylumbelliferyl 4-uanidinobenzoate hydrochloride as described(11). Michaelis-Menten kinetic analyses were performed by incubating a fixed concentration of active-site titrated proteinase

(400.4 nM MMP-1, 172.8 nM MMP-8, 9.01 nM MMP-13 and 1 nM matriptase) with 0-100 µM 2-Abz-SKGRSLIG-Y(NO_2) substrate. Assays were performed in a FLUOstar OPTIMA fluorimeter (BMG Labtech, Aylesbury, UK) at 37°C, λ_{ex} 320 nm, λ_{em} 420 nm, ensuring linearity of substrate hydrolysis prior to further quantification. Substrate hydrolysis was quantified using a standard curve representing total substrate hydrolysis at each concentration. Non-linear regression analysis was performed to generate kinetic constants K_M and V_{max} (GraphPad Prism Software), and k_{cat} calculated. Conditioned medium from an IL-1+OSM-stimulated bovine nasal cartilage explant cultures was generated as previously(12).

Calcium mobilisation assay — Following serum-starvation of SW1353 cells transduced in black-walled clear bottom 96-well plates, cells were washed with 200 µL Hank's Balanced Salt Solution supplemented with 20 mM HEPES, pH 7 and 2 mM $CaCl_2$ (HHBS/Ca^{2+}). To each well, 50 µL of a 5 µM stock solution of the calcium indicator Rhod-4 AM (Santa Cruz, Heidelberg, Germany) in HHBS/Ca^{2+} supplemented with 2.5 mM probenecid (Santa Cruz) and 0.02% pluronic F-127 (Thermo Fisher) was added and incubated at room temperature in the dark for 45 minutes. Cells were then washed with HHBS/Ca^{2+} before incubating at room temperature for 20 minutes in HHBS/Ca^{2+} to allow for dye de-esterification.

Assays were performed in a FLUOstar OPTIMA fluorimeter (BMG Labtech) at 37°C during which its injection pumps were each primed with 2 mL of HHBS/Ca^{2+}, before priming with 1 mL of test solutions. The test solution in pump A was always at 2x final concentration, whereas the test solution in pump B was at 3x final concentration. To perform the assay, each well was replaced with 30 µL HHBS/Ca^{2+}, and placed in the fluorimeter programmed to read in single-well mode (readings taken every second at λ_{ex} 520 nm and λ_{em} 590 nm). For each assay, a 10 second baseline was established before 30 µL injection from pump A, 90 seconds incubation followed by 30 µL injection from pump B.

Active Matrix Metalloproteinase-1 Production — Purified active MMP-1 was produced for cell culture work to avoid addition of APMA on cells. Recombinant human proMMP-1 was expressed in *Escherichia coli* and refolded from chaotrope-solubilised inclusion bodies as described previously(52). The refolded pro-enzyme was purified using an automated two-step procedure on an ÄKTAxpress system (GE Healthcare): 1) immobilised metal ion affinity chromatography (IMAC) using a Ni^{2+}-charged 5 mL HiTrap IMAC FF column with 50 mM Tris pH 7.4, 150 mM NaCl, 10 mM $CaCl_2$ (TNC) as binding buffer, and an elution buffer of TNC supplemented with 0.5 M imidazole; 2) size-exclusion chromatography (SEC) performed on a HiLoad 26/60 Superdex 75 prep grade column with TNC as running buffer. Following incubation with APMA and MMP-3(53), the activated MMP-1 was re-purified by tandem IMAC-SEC as above. Aliquots of 5 µM MMP-1 were lyophilised from TNC buffer supplemented with 1% (w/v) BSA and stored at -80°C until required.

Assessment of PAR2 receptor Antagonism — Lyophilised active MMP-1 was resuspended to 1 µM in DMEM-F12 medium supplemented with 10 mM $CaCl_2$ and subsequently added to cells for the required time. Matriptase or SLIGKV-NH_2 was added at twice the final concentration and cells incubated for the required time at 37°C prior to RNA extraction (see below).

Gene expression analyses — RNA was extracted from cells in a 96-well format using Cells-to-cDNA lysis buffer (Thermo Fisher) according to the manufacturer's instructions, prior to cDNA synthesis by MMLV reverse transcriptase (Thermo Fisher) according to manufacturer instructions. Real-time (q)PCR was performed using TaqMan Fast Advanced Master Mix with the following cycling conditions (QuantStudio 3, Thermo Fisher): 2 minutes at 50°C, 20 seconds at 95°C followed by 40 cycles of 1 second at 95°C, 20 seconds at 60°C. Primer and probe sequences for *MMP1*, *MMP13*(54), and *ATF3*(24) as previously described. *GAPDH* expression was measured using: Forward 5'-GTGAACCATGAGAAGTATGACAAC-3'; reverse 5'-CATGAGTCCTTCCACGATACC-3'; and probe Fam-CCTCAAGATCATCAGCAATGCCTCCTG-Tamra.

SDS-PAGE and Immunoblotting — Whole cell lysates were generated using RIPA buffer (150 mM sodium chloride, 1.0% Triton X-100,

0.5% sodium deoxycholate, 0.1% SDS, 50 mM Tris, pH 8.0, 10 mM sodium fluoride and 1 mM sodium orthovanadate, supplemented with a cOmplete Mini Protease Inhibitor Cocktail tablet). Samples were prepared and SDS-PAGE performed as previously(12). Proteins were transferred to PVDF membrane using a Trans-Blot SD Semi-Dry Transfer Cell (BioRad, Watford, UK) according to the manufacturer's instructions, and incubated with primary antibody overnight at 4°C. Antibodies used were: phospho-p38 (#4511), phospho-ERK1/2 (#9101), ERK1/2 (#9102) from Cell Signalling Technology (Danvers, USA) and p38 (SC-535) from Santa Cruz.

Enzyme-linked immunosorbent assay (ELISA) — Total MMP-1 was measured as previously described(55), whereas total MMP-13 was measured using a Human Total MMP-13 DuoSet ELISA kit (R&D Biosystems) according to the manufacturer's instructions.

Statistical analyses — Statistical differences between sample groups were assessed using the Student's 2-tailed unpaired *t*-test, where ***p<0.001, **p<0.01, *p<0.05. For clarity, only selected comparisons are presented in some figures.

Acknowledgments: We thank all the collaborators mentioned for the generous provision of reagents.

Conflict of interest: The authors declare that they have no conflicts of interest with the contents of this article.

REFERENCES

1. Barrett, A. J. and McDonald, J. K. (1986) Nomenclature: protease, proteinase and peptidase. *Biochem. J.* **237**, 935–935, 10.1042/bj2370935
2. Ugalde, A., Ordóñez, G., Quirós, P., Puente, X., and López-Otín, C. (2010) in *Matrix Metalloproteinase Protocols (Methods and Protocols)*, volume 622, pp. 3–29, Humana Press, Totowa, NJ
3. Lazarus, G., Daniels, J., Brown, R., Bladan, H., and Fullmer, H. (1968) Degradation of collagen by a human granulocyte collagenolytic system. *J. Clin. Investig.* **47**, 2622–2629, 10.1172/JCI105945
4. Ferrell, W. R., Lockhart, J. C., Kelso, E. B., Dunning, L., Plevin, R., Meek, S. E., Smith, A. J. H., Hunter, G. D., McLean, J. S., McGarry, F., Ramage, R., Jiang, L., Kanke, T., and Kawagoe, J. (2003) Essential role for proteinase-activated receptor-2 in arthritis. *J. Clin. Investig.* **111**, 35–41, 10.1172/jci200316913
5. Ferrell, W. R., Kelso, E. B., Lockhart, J. C., Plevin, R., and McInnes, I. B. (2010) Protease-activated receptor 2: a novel pathogenic pathway in a murine model of osteoarthritis. *Annals Rheum. Dis.* **69**, 2051–2054, 10.1136/ard.2010.130336
6. Huesa, C., Ortiz, A. C., Dunning, L., McGavin, L., Bennett, L., McIntosh, K., Crilly, A., Kurowska-Stolarska, M., Plevin, R., van't Hof, R. J., Rowan, A. D., McInnes, I. B., Goodyear, C. S., Lockhart, J. C., and Ferrell, W. R. (2016) Proteinase-activated receptor 2 modulates OA-related pain, cartilage and bone pathology. *Annals Rheum. Dis.* **75**, 1989–1997, 10.1136/annrheumdis-2015-208268
7. Kelso, E. B., Lockhart, J. C., Hembrough, T., Dunning, L., Plevin, R., Hollenberg, M. D., Sommerhoff, C. P., McLean, J. S., and Ferrell, W. R. (2006) Therapeutic promise of proteinase-activated receptor-2 antagonism in joint inflammation. *J. Pharmacol. Exp. Ther.* **316**, 1017–1024, 10.1124/jpet.105.093807
8. Amiable, N., Martel-Pelletier, J., Lussier, B., Tat, S. K., Pelletier, J.-P., and Boileau, C. (2011) Proteinase-activated receptor-2 gene disruption limits the effect of osteoarthritis on cartilage in mice: A novel target in joint degradation. *J. Rheumatol.* **38**, 911–920, 10.3899/jrheum.100710
9. Jackson, M. T., Moradi, B., Zaki, S., Smith, M. M., McCracken, S., Smith, S. M., Jackson, C. J., and Little, C. B. (2014) Depletion of protease-activated receptor 2 but not protease-activated receptor 1 may confer protection against osteoarthritis in mice through extracartilaginous mechanisms. *Arthritis & Rheumatol.* **66**, 3337–3348, 10.1002/art.38876
10. Milner, J. M., Patel, A., Davidson, R. K., Swingler, T. E., Desilets, A., Young, D. A., Kelso, E. B., Donell, S. T., Cawston, T. E., Clark, I. M., Ferrell, W. R., Plevin, R., Lockhart, J. C., Leduc, R., and Rowan, A. D. (2010) Matriptase is a novel initiator of cartilage matrix degradation in osteoarthritis. *Arthritis Rheum.* **62**, 1955–1966, 10.1002/art.27476
11. Wilkinson, D. J., Habgood, A., Lamb, H. K., Thompson, P., Hawkins, A. R., Desilets, A., Leduc, R., Steinmetzer, T., Hammami, M., Lee, M. S., Craik, C. S., Watson, S., Lin, H., Milner, J. M., and Rowan, A. D. (2017) Matriptase induction of metalloproteinase-dependent aggrecanolysis in vitro and in vivo promotion of osteoarthritic cartilage damage by multiple mechanisms. *Arthritis & Rheumatol.* **69**, 1601–1611, 10.1002/art.40133
12. Wilkinson, D. J., Desilets, A., Lin, H., Charlton, S., Arques, M. D., Falconer, A., Bullock, C., Hsu, Y. C., Birchall, K., Hawkins, A., Thompson, P., Ferrell, W. R., Lockhart, J., Plevin, R., Zhang, Y. D., et al. (2017) The serine proteinase hepsin is an activator of pro-matrix metalloproteinases: molecular mechanisms and implications for extracellular matrix turnover. *Sci. Reports* **7**, 10.1038/s41598-017-17028-3
13. Wilkinson, D. J., Arques, M. C., Huesa, C., and Rowan, A. D. (2019) Serine proteinases in the turnover of the cartilage extracellular matrix in the joint: implications for therapeutics. *Br. J. Pharmacol.* **176**, 38–51, 10.1111/bph.14173
14. Hollenberg, M. D., Mihara, K., Polley, D., Suen, J. Y., Han, A., Fairlie, D. P., and Ramachandran,

R. (2014) Biased signalling and proteinase-activated receptors (PARs): targeting inflammatory disease. *Br. J. Pharmacol.* **171**, 1180–1194, 10.1111/bph.12544

15. Oikonomopoulou, K., Diamandis, E. P., Hollenberg, M. D., and Chandran, V. (2018) Proteinases and their receptors in inflammatory arthritis: an overview. *Nat. Rev. Rheumatol.* **14**, 170–180, 10.1038/nrrheum.2018.17
16. Bonnans, C., Chou, J., and Werb, Z. (2014) Remodelling the extracellular matrix in development and disease. *Nat. Rev. Mol. Cell Biol.* **15**, 786–801, 10.1038/nrm3904
17. Ramachandran, R., Mihara, K., Chung, H., Renaux, B., Lau, C. S., Muruve, D. A., DeFea, K. A., Bouvier, M., and Hollenberg, M. D. (2011) Neutrophil elastase acts as a biased agonist for proteinase-activated receptor-2 (PAR2). *J. Biol. Chem.* **286**, 24638–24648, 10.1074/jbc.M110.201988
18. Zhao, P., Lieu, T., Barlow, N., Metcalf, M., Veldhuis, N. A., Jensen, D. D., Kocan, M., Sostegni, S., Haerteis, S., Baraznenok, V., Henderson, I., Lindstrom, E., Guerrero-Alba, R., Valdez-Morales, E. E., Liedtke, W., et al. (2014) Cathepsin S causes inflammatory pain via biased agonism of PAR2 and TRPV4. *J. Biol. Chem.* **289**, 27215–27234, 10.1074/jbc.M114.599712
19. Zhao, P., Metcalf, M., and Bunnett, N. W. (2014) Biased signaling of protease-activated receptors. *Front. endocrinology* **5**, 67–67, 10.3389/fendo.2014.00067
20. Cawston, T. E., Ellis, A. J., Humm, G., Lean, E., Ward, D., and Curry, V. (1995) Interleukin-1 and oncostatin M in combination promote the release of collagen fragments from bovine nasal cartilage in culture. *Biochem. Biophys. Res. Commun.* **215**, 377–385, 10.1006/bbrc.1995.2476
21. Cawston, T. E., Curry, V. A., Summers, C. A., Clark, I. M., Riley, G. P., Life, P. F., Spaull, J. R., Goldring, M. B., Koshy, P. J. T., Rowan, A. D., and Shingleton, W. D. (1998) The role of oncostatin M in animal and human connective tissue collagen turnover and its localization within the rheumatoid joint. *Arthritis Rheum.* **41**, 1760–1771, 10.1002/1529-0131(199810)41:10<1760::aid-art8>3.0.co;2-m
22. Boileau, C., Amiable, N., Martel-Pelletier, J., Fahmi, H., Duval, N., and Pelletier, J.-P. (2007) Activation of proteinase-activated receptor 2 in human osteoarthritic cartilage upregulates catabolic and proinflammatory pathways capable of inducing cartilage degradation: a basic science study. *Arthritis Res. & Ther.* **9**, 10.1186/ar2329
23. Xiang, Y., Masuko-Hongo, K., Sekine, T., Nakamura, H., Yudoh, K., Nishioka, K., and Kato, T. (2006) Expression of proteinase-activated receptors PAR-2 in articular chondrocytes is modulated by IL-1 beta, TNF-alpha and TGF-beta. *Osteoarthr. Cartil.* **14**, 1163–1173, 10.1016/j.joca.2006.04.015
24. Chan, C. M., Macdonald, C. D., Litherland, G. J., Wilkinson, D. J., Skelton, A., Europe-Finner, G. N., and Rowan, A. D. (2017) Cytokine-induced MMP13 expression in human chondrocytes is dependent on activating transcription factor 3 (ATF3) regulation. *J. Biol. Chem.* **292**, 1625–1636, 10.1074/jbc.M116.756601
25. Tanaka, Y., Sekiguchi, F., Hong, H., and Kawabata, A. (2008) PAR2 triggers IL-8 release via MEK/ERK and PI3-kinase/Akt pathways in GI epithelial cells. *Biochem. Biophys. Res. Commun.* **377**, 622–626, 10.1016/j.bbrc.2008.10.018
26. Ungefroren, H., Witte, D., Fiedler, C., Gadeken, T., Kaufmann, R., Lehnert, H., Gieseler, F., and Rauch, B. H. (2017) The role of PAR2 in TGF-beta 1-induced ERK activation and cell motility. *Int. J. Mol. Sci.* **18**, 10.3390/ijms18122776
27. Pan, S. L., Tao, K. Y., Guh, J. H., Sun, H. L., Huang, D. Y., Chang, Y. L., and Teng, C. M. (2008) The p38 mitogen-activated protein kinase pathway plays a critical role in PAR2-induced endothelial IL-8 production and leukocyte adhesion. *Shock* **30**, 496–502, 10.1097/SHK.0b013e3181673233
28. Turk, B. E., Huang, L. L., Piro, E. T., and Cantley, L. C. (2001) Determination of protease cleavage site motifs using mixture-based oriented peptide libraries. *Nat. Biotechnol.* **19**, 661–667,

10.1038/90273

29. Netzelarnett, S., Fields, G., Birkedalhansen, H., and Vanwart, H. E. (1991) Sequence specificities of human fibroblast and neutrophil collagenases. *J. Biol. Chem.* **266**, 6747–6755
30. Rawlings, N. D., Barrett, A. J., and Finn, R. (2016) Twenty years of the merops database of proteolytic enzymes, their substrates and inhibitors. *Nucleic Acids Res.* **44**, D343–D350, 10.1093/nar/gkv1118
31. Molino, M., Barnathan, E. S., Numerof, R., Clark, J., Dreyer, M., Cumashi, A., Hoxie, J. A., Schechter, N., Woolkalis, M., and Brass, L. F. (1997) Interactions of mast cell tryptase with thrombin receptors and PAR-2. *J. Biol. Chem.* **272**, 4043–4049
32. Camerer, E., Barker, A., Duong, D. N., Ganesan, R., Kataoka, H., Cornelissen, I., Darragh, M. R., Hussain, A., Zheng, Y.-W., Srinivasan, Y., Brown, C., Xu, S.-M., Regard, J. B., Lin, C.-Y., Craik, C. S., et al. (2010) Local protease signaling contributes to neural tube closure in the mouse embryo. *Dev. Cell* **18**, 25–38, 10.1016/j.devcel.2009.11.014
33. Beliveau, F., Desilets, A., and Leduc, R. (2009) Probing the substrate specificities of matriptase, matriptase-2, hepsin and DESC1 with internally quenched fluorescent peptides. *Febs J.* **276**, 2213–2226, 10.1111/j.1742-4658.2009.06950.x
34. Nagase, H. and Visse, R. (2011) in *Extracellular Matrix Degradation*, volume 2, book section 5, pp. 95–122
35. Swingler, T. E., Waters, J. G., Davidson, R. K., Pennington, C. J., Puente, X. S., Darrah, C., Cooper, A., Donell, S. T., Guile, G. R., Wang, W. J., and Clark, I. M. (2009) Degradome expression profiling in human articular cartilage. *Arthritis Res. & Ther.* **11**, 10.1186/ar2741
36. Kevorkian, L., Young, D. A., Darrah, C., Donell, S. T., Shepstone, L., Porter, S., Brockbank, S. M. V., Edwards, D. R., Parker, A. E., and Clark, I. M. (2004) Expression profiling of metalloproteinases and their inhibitors in cartilage. *Arthritis Rheum.* **50**, 131–141, 10.1002/art.11433
37. Davidson, R. K., Waters, J. G., Kevorkian, L., Darrah, C., Cooper, A., Donell, S. T., and Clark, I. M. (2006) Expression profiling of metalloproteinases and their inhibitors in synovium and cartilage. *Arthritis Res. & Ther.* **8**, 10.1186/ar2013
38. Dulon, S., Cande, C., Bunnett, N. W., Hollenberg, M. D., Chignard, M., and Pidard, D. (2003) Proteinase-activated receptor-2 and human lung epithelial cells - disarming by neutrophil serine proteinases. *Am. J. Respir. Cell Mol. Biol.* **28**, 339–346, 10.1165/rcmb.4908
39. Trivedi, V., Boire, A., Tchemychev, B., Kaneider, N. C., Leger, A. J., O'Callaghan, K., Covic, L., and Kuliopulos, A. (2009) Platelet matrix metalloprotease-1 mediates thrombogenesis by activating PAR1 at a cryptic ligand site. *Cell* **137**, 332–343, 10.1016/j.cell.2009.02.018
40. Jaffre, F., Friedman, A. E., Hu, Z., Mackman, N., and Blaxall, B. C. (2012) beta-adrenergic receptor stimulation transactivates protease-activated receptor 1 via matrix metalloproteinase 13 in cardiac cells. *Circulation* **125**, 2993–3003, 10.1161/circulationaha.111.066787
41. Li, X. and Tai, H.-H. (2014) Thromboxane A(2) receptor-mediated release of matrix metalloproteinase-1 (MMP-1) induces expression of monocyte chemoattractant protein-1 (MCP-1) by activation of protease-activated receptor 2 (PAR2) in A549 human lung adenocarcinoma cells. *Mol. Carcinog.* **53**, 659–666, 10.1002/mc.22020
42. Das, K., Prasad, R., Ansari, S. A., Roy, A., Mukherjee, A., and Sen, P. (2018) Matrix metalloproteinase-2: A key regulator in coagulation proteases mediated human breast cancer progression through autocrine signaling. *Biomed. & Pharmacother.* **105**, 395–406, 10.1016/j.biopha.2018.05.155
43. Suen, J. Y., Gardiner, B., Grimmond, S., and Fairlie, D. P. (2010) Profiling gene expression induced by protease-activated receptor 2 (PAR2) activation in human kidney cells. *Plos One* **5**, 10.1371/journal.pone.0013809
44. Vliagoftis, A., Schwingshackl, A., Milne, C. D., Duszyk, M., Hollenberg, M. D., Wallace,

J. L., Befus, A. D., and Moqbel, R. (2000) Proteinase-activated receptor-2-mediated matrix metalloproteinase-9 release from airway epithelial cells. *J. Allergy Clin. Immunol.* **106**, 537–545, 10.1067/mai.2000.109058

45. Ramachandran, R., Mihara, K., Mathur, M., Rochdi, M. D., Bouvier, M., Defea, K., and Hollenberg, M. D. (2009) Agonist-biased signaling via proteinase activated receptor-2: Differential activation of calcium and mitogen-activated protein kinase pathways. *Mol. Pharmacol.* **76**, 791–801, 10.1124/mol.109.055509
46. Al-Ani, B., Hansen, K. K., and Hollenberg, M. D. (2004) Proteinase-activated receptor-2: Key role of amino-terminal dipeptide residues of the tethered ligand for receptor activation. *Mol. Pharmacol.* **65**, 149–156, 10.1124/mol.65.1.149
47. Al-Ani, B., Wijesuriya, S. J., and Hollenberg, M. D. (2002) Proteinase-activated receptor 2: Differential activation of the receptor by tethered ligand and soluble peptide analogs. *J. Pharmacol. Exp. Ther.* **302**, 1046–1054, 10.1124/jpet.302.3.1046
48. Barksby, H. E., Milner, J. M., Patterson, A. M., Peake, N. J., Hui, W., Robson, T., Lakey, R., Middleton, J., Cawston, T. E., Richards, C. D., and Rowan, A. D. (2006) Matrix metalloproteinase 10 promotion of collagenolysis via procollagenase activation - implications for cartilage degradation in arthritis. *Arthritis Rheum.* **54**, 3244–3253, 10.1002/art.22167
49. Schaegger, H. (2006) Tricine-SDS-PAGE. *Nat. Protoc.* **1**, 16–22, 10.1038/nprot.2006.4
50. Cowell, J., Buck, M., Essa, A. H., Clarke, R., Vollmer, W., Vollmer, D., Hilkens, C. M., Isaacs, J. D., Hall, M. J., and Gray, J. (2017) Traceless cleavage of protein-biotin conjugates under biologically compatible conditions. *Chembiochem* **18**, 1688–1691, 10.1002/cbic.201700214
51. Willenbrock, F., Crabbe, T., Slocombe, P. M., Sutton, C. W., Docherty, A. J. P., Cockett, M. I., Oshea, M., Brocklehurst, K., Phillips, I. R., and Murphy, G. (1993) The activity of the tissue inhibitors of metalloproteinases is regulated by c-terminal domain interactions: A kinetic analysis of the inhibition of gelatinase a. *Biochemistry* **32**, 4330–4337, 10.1021/bi00067a023
52. Arnold, L. H., Butt, L. E., Prior, S. H., Read, C. M., Fields, G. B., and Pickford, A. R. (2011) The interface between catalytic and hemopexin domains in matrix metalloproteinase-1 conceals a collagen binding exosite. *J. Biol. Chem.* **286**, 45073–45082, 10.1074/jbc.M111.285213
53. Chung, L. D., Dinakarpandian, D., Yoshida, N., Lauer-Fields, J. L., Fields, G. B., Visse, R., and Nagase, H. (2004) Collagenase unwinds triple-helical collagen prior to peptide bond hydrolysis. *Embo J.* **23**, 3020–3030, 10.1038/sj.emboj.7600318
54. Litherland, G. J., Elias, M. S., Hui, W., Macdonald, C. D., Catterall, J. B., Barter, M. J., Farren, M. J., Jefferson, M., and Rowan, A. D. (2010) Protein kinase C isoforms zeta and iota mediate collagenase expression and cartilage destruction via STAT3-and ERK-dependent c-fos induction. *J. Biol. Chem.* **285**, 22414–22425, 10.1074/jbc.M110.120121
55. Clark, I. M., Powell, L. K., Wright, J. K., Cawston, T. E., and Hazleman, B. L. (1992) Monoclonal antibodies against human fibroblast collagenase and the design of an enzyme-linked immunosorbent assay to measure total collagenase. *Matrix* **12**, 475–480, 10.1016/s0934-8832(11)80092-2

FOOTNOTES

This work was supported by Fight Arthritis in the North East (FARNE), the JGWP Foundation, and Arthritis Research UK (Grant 20199).

The abbreviations used are: 2-Abz, 2-aminobenzoic acid; AFU, arbitrary fluorescence units; APMA, 4-aminophenylmercuric acetate; DFP, Diisopropyl fluorophosphate; GPCR, G-protein coupled receptor; MMP, Matrix Metalloproteinase; PAR2, proteinase-activated receptor 2; PVDF, Polyvinylidene fluoride.

FIGURES

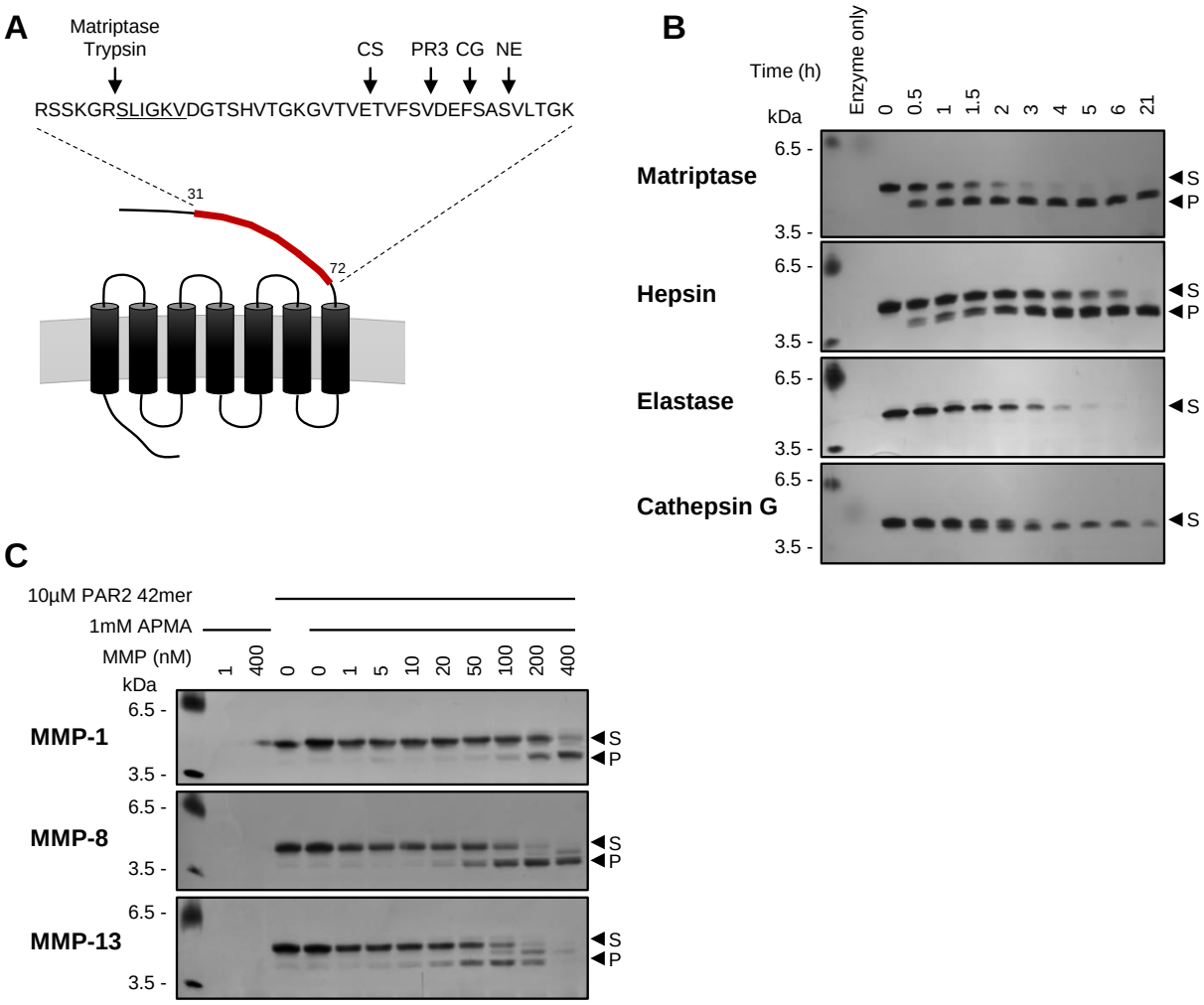

Figure 1: The collagenases are able to cleave the PAR2 extracellular domain. A 42 amino acid peptide corresponding to Arg^{31}-Lys^{72} of the extracellular domain of PAR2 (denoted in red) was produced. Various known cleavage sites are highlighted: the canonical activation site (trypsin, matriptase etc., with the tethered ligand/activator peptide sequence underlined); CS = cathepsin S; PR3 = proteinase 3; CG = cathepsin G; NE = neutrophil elastase (A). The $PAR2^{31-72}$ peptide (10 μM) was incubated with 10 nM of hepsin or elastase, or 1 nM cathepsin G, or 0.1 nM matriptase for the indicated durations before resolving on 20% polyacrylamide gels utilising a Tris-Tricine buffer system and silver staining. S = substrate, P = product. Presented gels are representative of at least two independent experiments (B). The $PAR2^{31-72}$ peptide (10 μM) was incubated with increasing concentrations of APMA-activated recombinant proMMP-1, -8 and -13 for 24 hours before resolving on 20% polyacrylamide gels utilising a Tris-Tricine buffer system and silver staining. S = substrate, P = product. The presented gels are representative of three independent experiments (C).

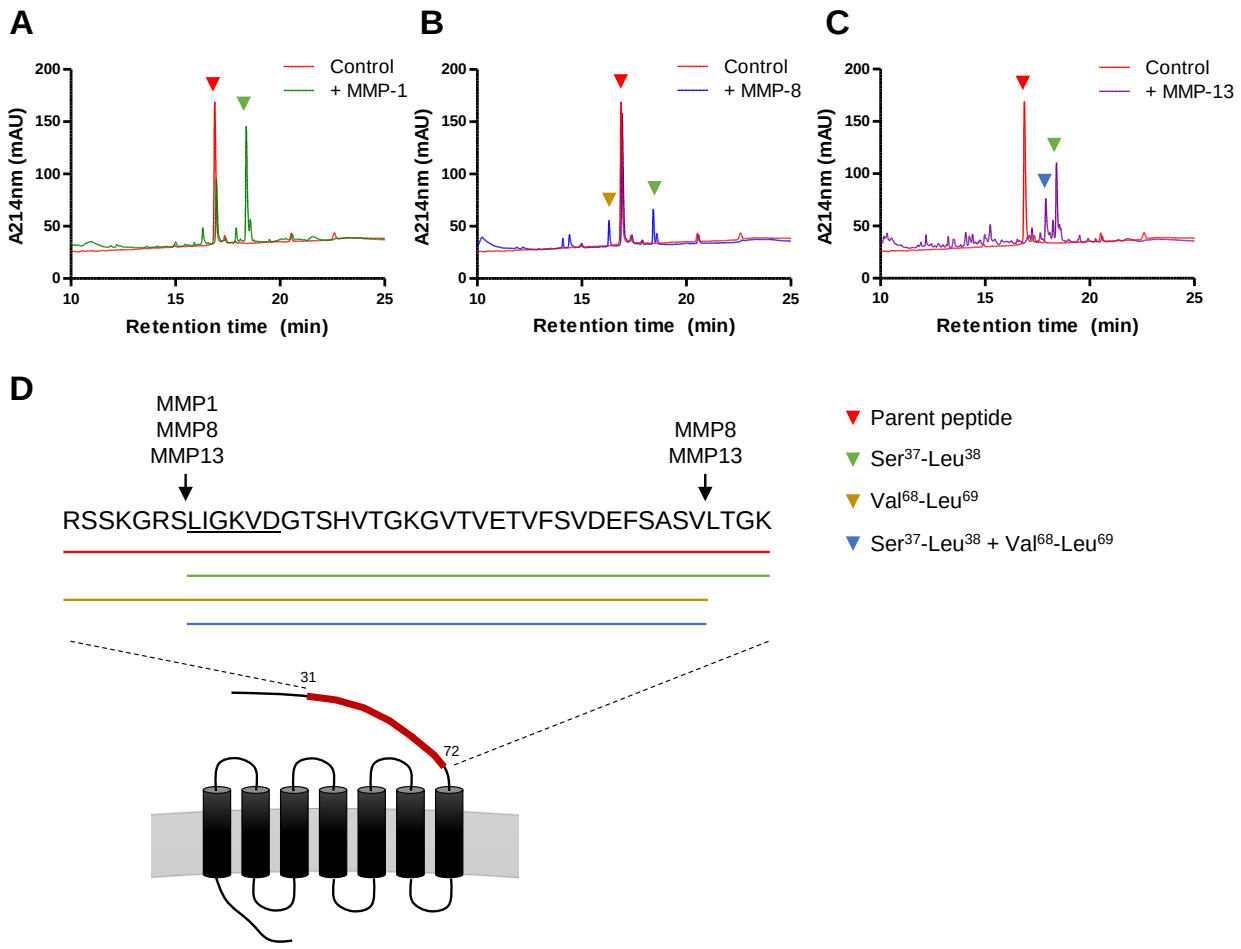

Figure 2: The MMP collagenases cleave PAR2 at a novel site. The PAR2$^{31-72}$ peptide (10 μM) was incubated with APMA-activated MMP-1 (400 nM; A), MMP-8 (20 nM; B) or MMP-13 (200 nM; C) for 24 hours and reversed-phase HPLC performed. HPLC chromatograms are representative of at least two independent experiments, and are presented as separate graphs for clarity with the same control chromatogram presented in each panel. Peaks identified by HPLC were collected and subjected to further analysis by electrospray MS, which identified MMP-derived cleavage sites at Ser^{37}-Leu^{38} and Val^{68}-Leu^{69}, to reveal a putative neo-epitope tethered ligand (underlined in D). The coloured arrows (A-C) and lines (D) indicate the following: red = parent peptide; green = Ser^{37}-Leu^{38} cleavage; amber = Val^{68}-Leu^{69} cleavage; blue = Ser^{37}-Leu^{38} and Val^{68}-Leu^{69} cleavage. Observed masses are presented in Supporting Table S1.

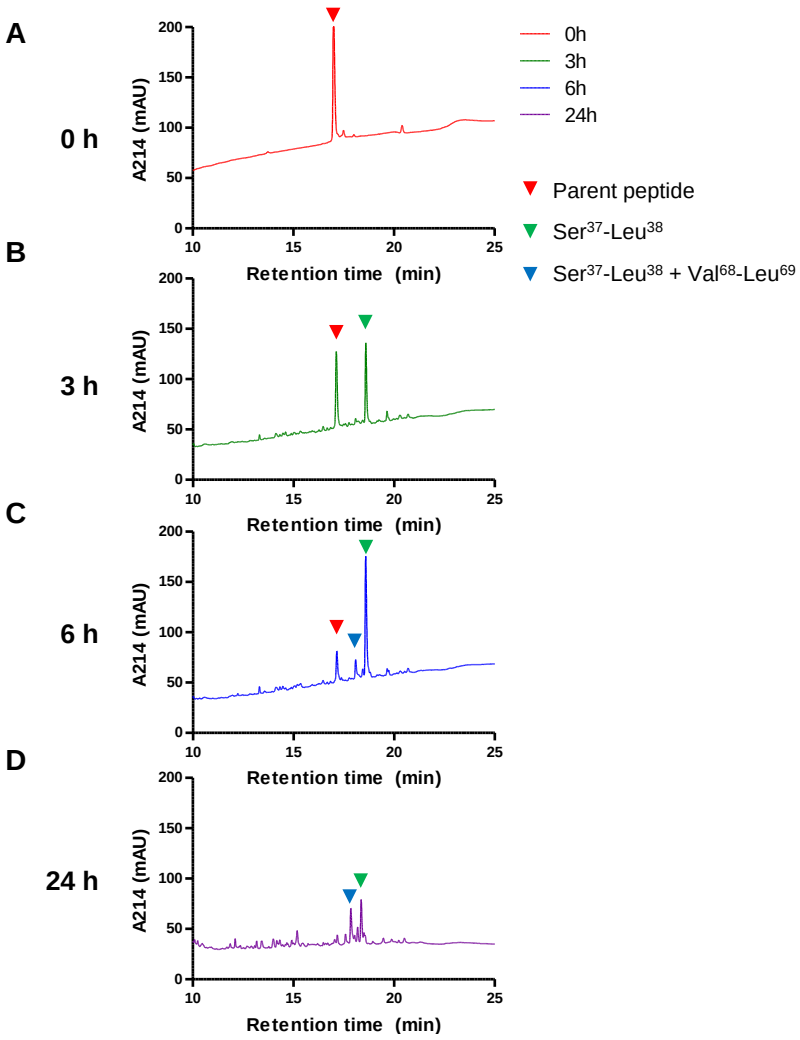

Figure 3: Time-course of PAR2$^{31-72}$ cleavage by MMP-13. PAR2$^{31-72}$ peptide (10 µM) was incubated with APMA-activated proMMP-13 (200 nM) over a 24 hour timecourse as indicated (A-D), and reversed-phase HPLC performed. Arrows indicate identity of observed peaks: red = parent peptide; green = Ser^{37}-Leu^{38}; blue = Ser^{37}-Leu^{38} + Val^{68}-Leu^{69}. Presented HPLC chromatograms are representative of three independent experiments.

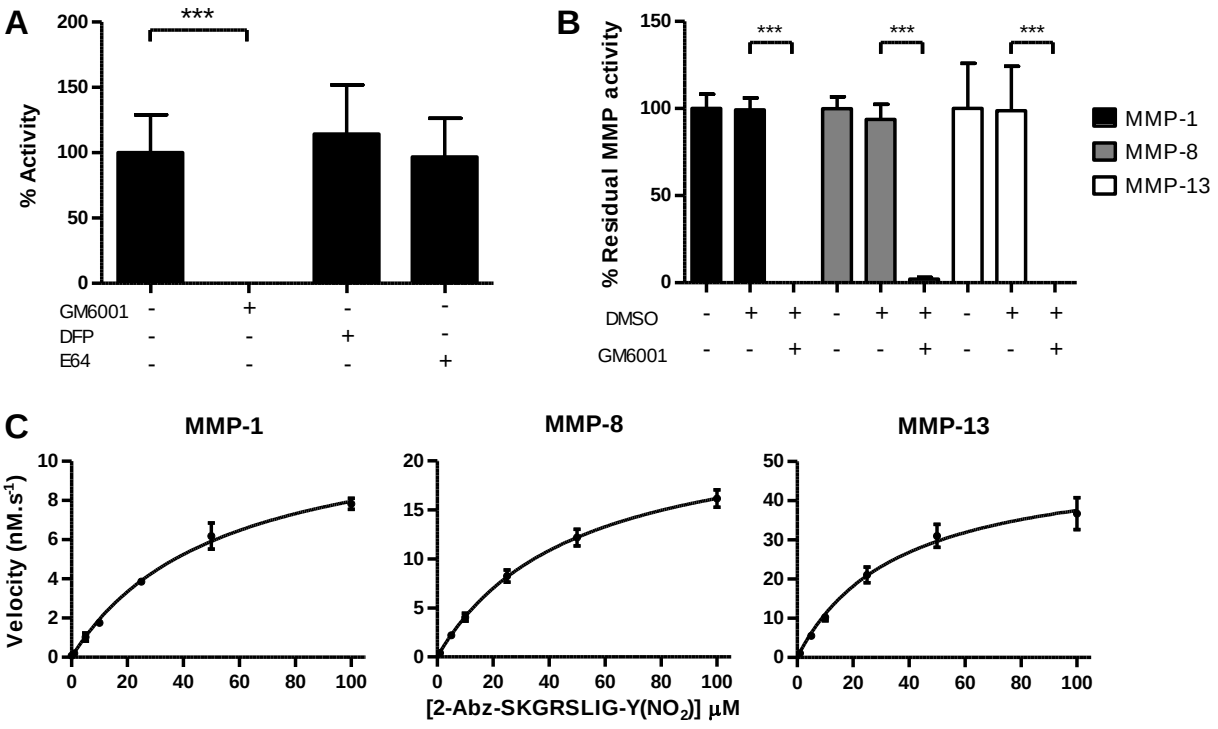

D

Enzyme	k_{cat} (min^{-1})	K_M (µM)	k_{cat}/K_M ($M^{-1}.s^{-1}$)
MMP-1	0.03 ± 0.002	52.64 ± 6.30	0.09 x 10^2
MMP-8	0.14 ± 0.010	49.05 ± 6.64	0.47 x 10^2
MMP-13	5.62 ± 0. 69	36.03 ± 2.93	2.6 x 10^3
Matriptase	1722 ± 253.8	46.62 ± 4.12	6.16 x 10^5

Figure 4: The collagenases cleave PAR2 with varying efficiencies. 2-Abz-SKGRSLIG-Y(NO_2) peptide (10 µM) was incubated with day 14 conditioned media from IL-1+OSM-stimulated bovine nasal cartilage explant cultures in the presence or absence of 100 µM GM6001, 10 µM E64 or 2 mM DFP. Data (mean ± S.D.) are normalised to the no inhibitor control sample and are representative of at least two independent experiments with conditioned media from different cartilages (A). 2-Abz-SKGRSLIG-Y(NO_2) peptide (50 µM) was incubated with APMA-activated recombinant proMMP-1 (50 nM), -8 (10 nM) or -13 (20 nM) in the presence or absence of 50 µM GM6001 or DMSO-only control, and data normalised to the inhibitor/DMSO negative sample (mean ± S.D.), combining means (each with *n*=2 technical replicates) from four independent experiments (B). Michaelis-Menten curves (mean ± S.D.; presented graphs show combined means (each with *n*=2 technical replicates) of three independent experiments) were generated using TIMP-1-titrated APMA-activated recombinant proMMP-1, -8 and -13 (C). The hydrolysis of substrate was quantified ($nM.s^{-1}$) using a standard curve determined by total substrate hydrolysis, and non-linear regression analysis performed to generate kinetic constants K_M and V_{max}. k_{cat} was subsequently calculated from V_{max} and active enzyme concentration. Tabulated kinetic constants (mean ± S.D.) are from three independent experiments. Matriptase kinetic parameters included for comparison (D). Selected statistical comparisons performed using student's two-tailed unpaired *t* tests, where ***, p<0.001.

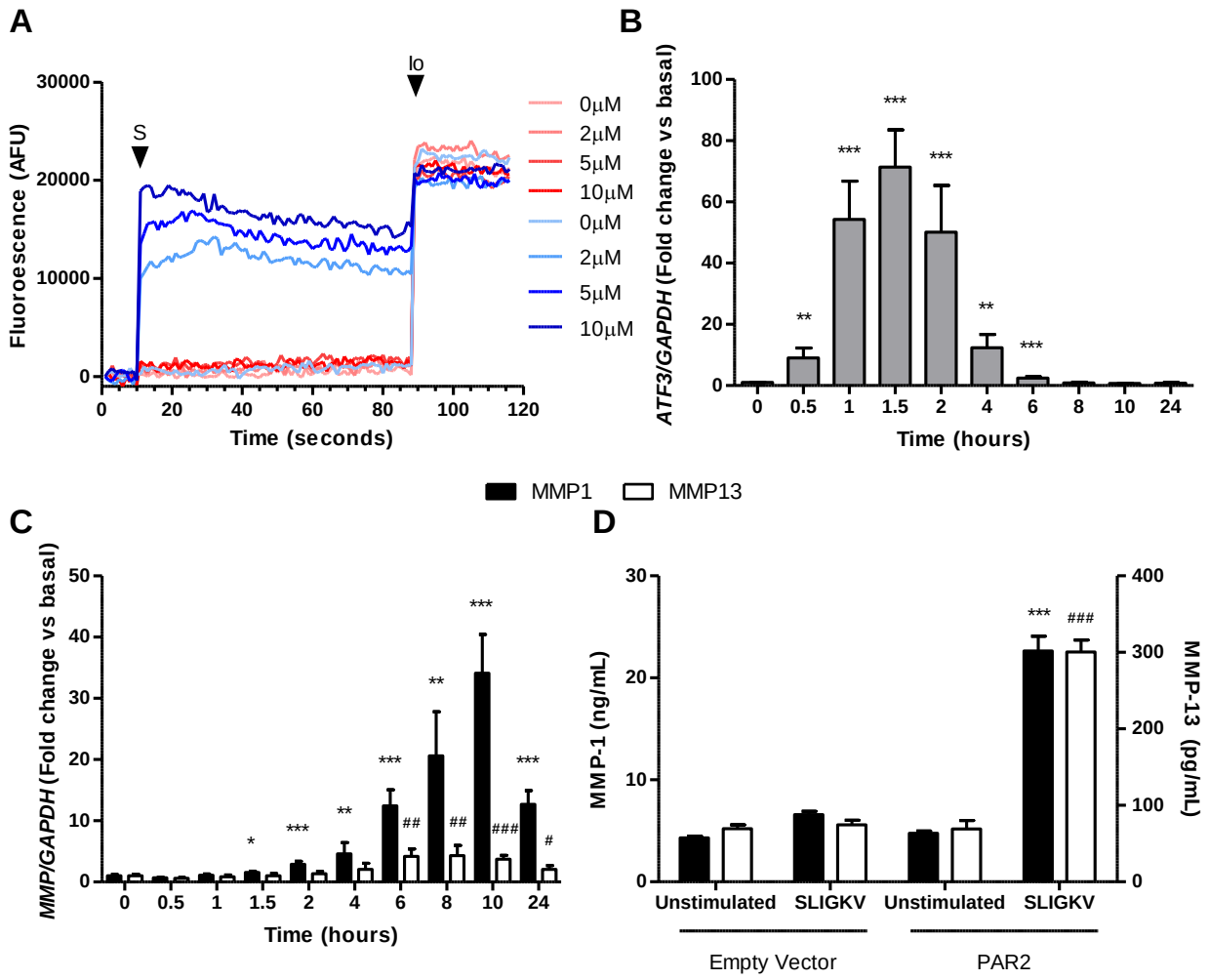

Figure 5: Activation of PAR2 by the canonical activator peptide SLIGKV-NH_2 results in *MMP1*, *MMP13* and *ATF3* expression. SW1353-PAR2 cells (blue lines) or empty vector control cells (red lines) loaded with Rhod-4-AM fluorescent calcium probe were subjected to titrations of 0-10 μM SLIGKVD-NH_2 (injected at arrow S) followed by 5 μM ionomycin (injected at arrow Io) and calcium mobilisation measured. Data are presented relative to basal fluorescence (at 0 seconds) and are representative of two independent experiments (each with *n*=3 technical replicates) (A). SW1353-PAR2 cells were stimulated with 100 μM SLIGKV-NH_2 for the indicated times and RT-qPCR performed for *ATF3* (B), *MMP1* and *MMP13* (C). Data are expressed relative to *GAPDH* and presented as fold-change compared with basal expression (mean ± S.D., *n*=4), representative of two independent experiments. SW1353-PAR2 or empty vector control cells were stimulated with 100 μM SLIGKV-NH_2 for 48 hours, and the conditioned medium used to perform MMP-1 and MMP-13 ELISAs. Data presented as mean ± S.D., representative of three independent experiments (each with *n*=6 technical replicates) (D). Selected statistical comparisons performed using student's two-tailed unpaired *t* tests against basal (unstimulated), where ***, p <0.001; **, p <0.01; *, p <0.05 for *MMP1* and *ATF3*; and ###, p <0.001; ##, p <0.01; #, p <0.05 for *MMP13*.

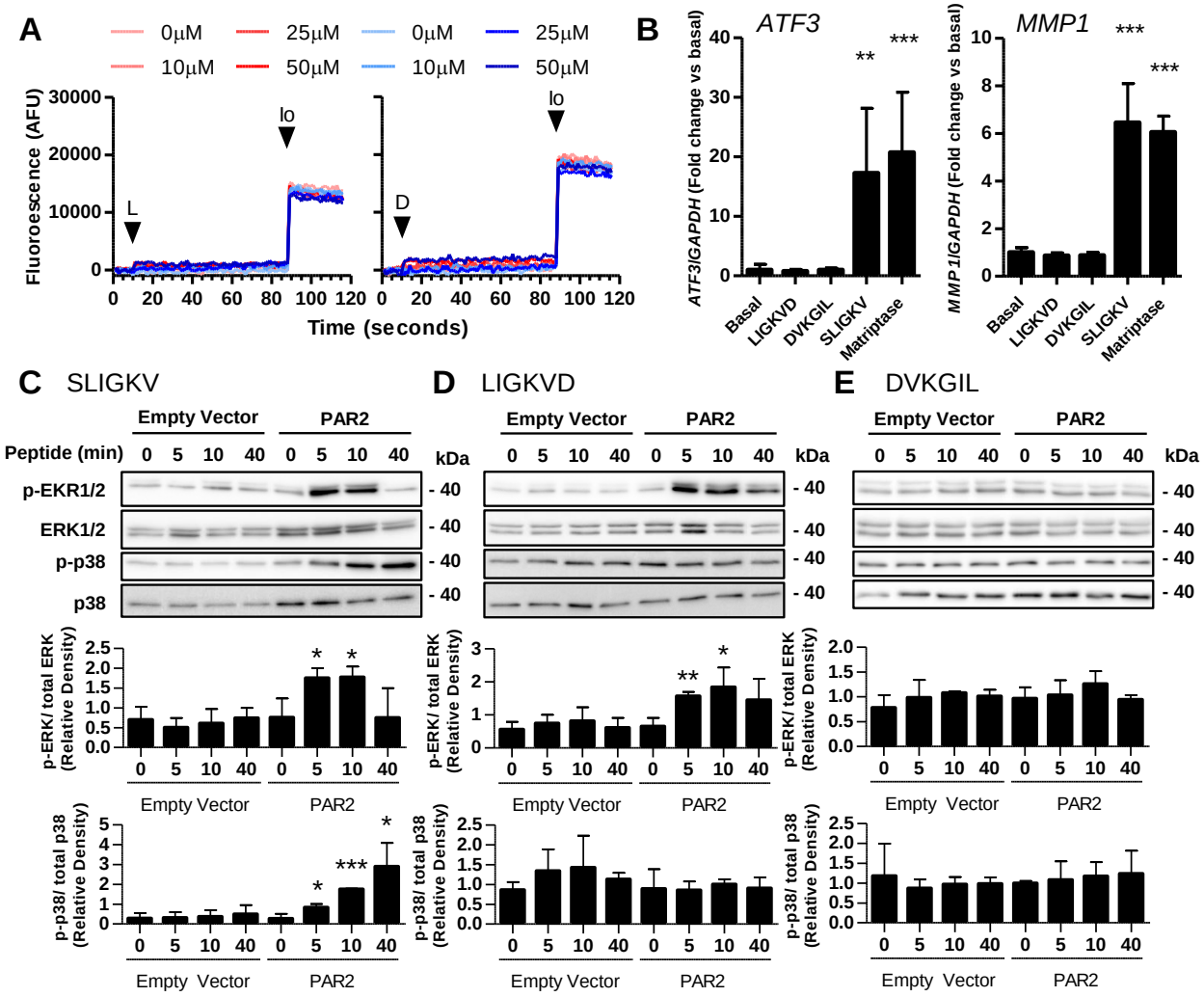

Figure 6: LIGKVD-NH_2 is not a canonical PAR2 activator. SW1353-PAR2 cells (blue lines) or empty vector control cells (red lines) loaded with Rhod-4-AM fluorescent calcium probe were subjected to titrations of 0-100 μM LIGKVD-NH_2 (left panel) or DVKGIL-NH_2 (right panel), injected at arrow L or D, respectively, followed by 5 μM ionomycin (injected at arrow Io) and calcium mobilisation measured. Data are presented relative to basal fluorescence (at 0 seconds) and are representative of two independent experiments (each with n=3 technical replicates) (A). SW1353-PAR2 cells were stimulated with 100 μM SLIGKV-NH_2, 100 μM LIGKVD-NH_2, 100 μM DVKGIL-NH_2 or 50 nM matriptase for 90 minutes (left panel) or 24 hours (right panel) and RT-qPCR performed for *ATF3* or *MMP1*. Data are expressed relative to *GAPDH* and presented as fold-change compared with basal expression (mean ± S.D., *n*=6), representative of three independent experiments (B). SW1353-PAR2 or empty vector control cells were stimulated with 100 μM SLIGKV-NH_2 (C), 100 μM LIGKVD-NH_2 (D) or 100 μM DVKGIL-NH_2 (E) for the indicated times and then cell lysates immunoblotted for phospho-ERK1/2, ERK1/2, phospho-p38 or p38. Combined densitometric scans of three independent experiments (mean ± S.D.) are presented. Statistical comparisons performed using student's two-tailed unpaired *t* tests comparing stimulated cells with basal, where ***, p <0.001; **, p <0.01; *, p <0.05.

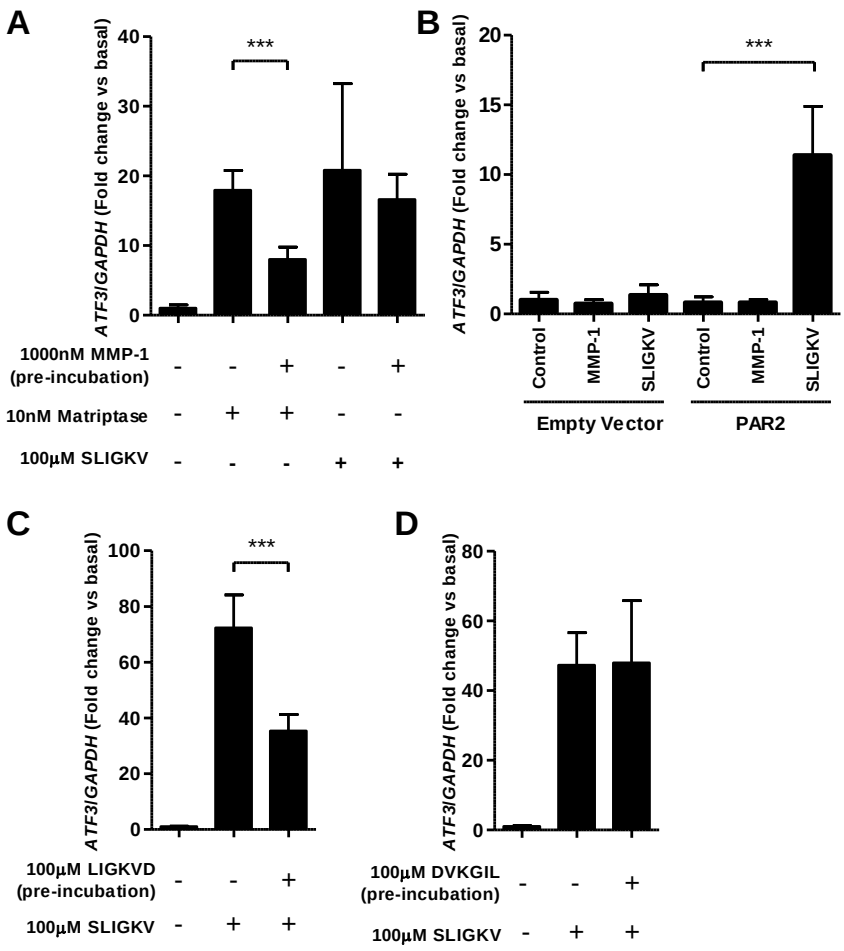

Figure 7: MMP1 is antagonistic to canonical PAR2 activation. SW1353-PAR2 cells were pre-treated with either 1000 nM active MMP-1 or serum-free medium (SFM) for 120 minutes prior to the addition of 10 nM matriptase or 100 µM SLIGKV-NH_2 for an additional 60 minutes and RT-qPCR performed for *ATF3* (A). SW1353-PAR2 or empty vector control cells were stimulated with either 1000 nM active MMP-1 or 100 µM SLIGKV-NH_2 for 60 minutes and RT-qPCR performed for *ATF3* (B). SW1353-PAR2 cells were pre-treated with 100 µM LIGKVD-NH_2 or SFM for 120 minutes prior to the addition of 100 µM SLIGKV-NH_2 for an additional 60 minutes and RT-qPCR performed for *ATF3* (C). SW1353-PAR2 cells were pre-treated with 100 µM DVKGIL-NH_2 or SFM for 120 minutes prior to the addition of 100 µM SLIGKV-NH_2 for an additional 60 minutes and RT-qPCR performed for *ATF3* (D). Data are expressed relative to *GAPDH* and presented as fold-change compared with basal expression (mean ± S.D., *n*=6), representative of at least three independent experiments. Selected statistical comparisons performed using student's two-tailed unpaired *t* tests, where ***, $p < 0.001$.

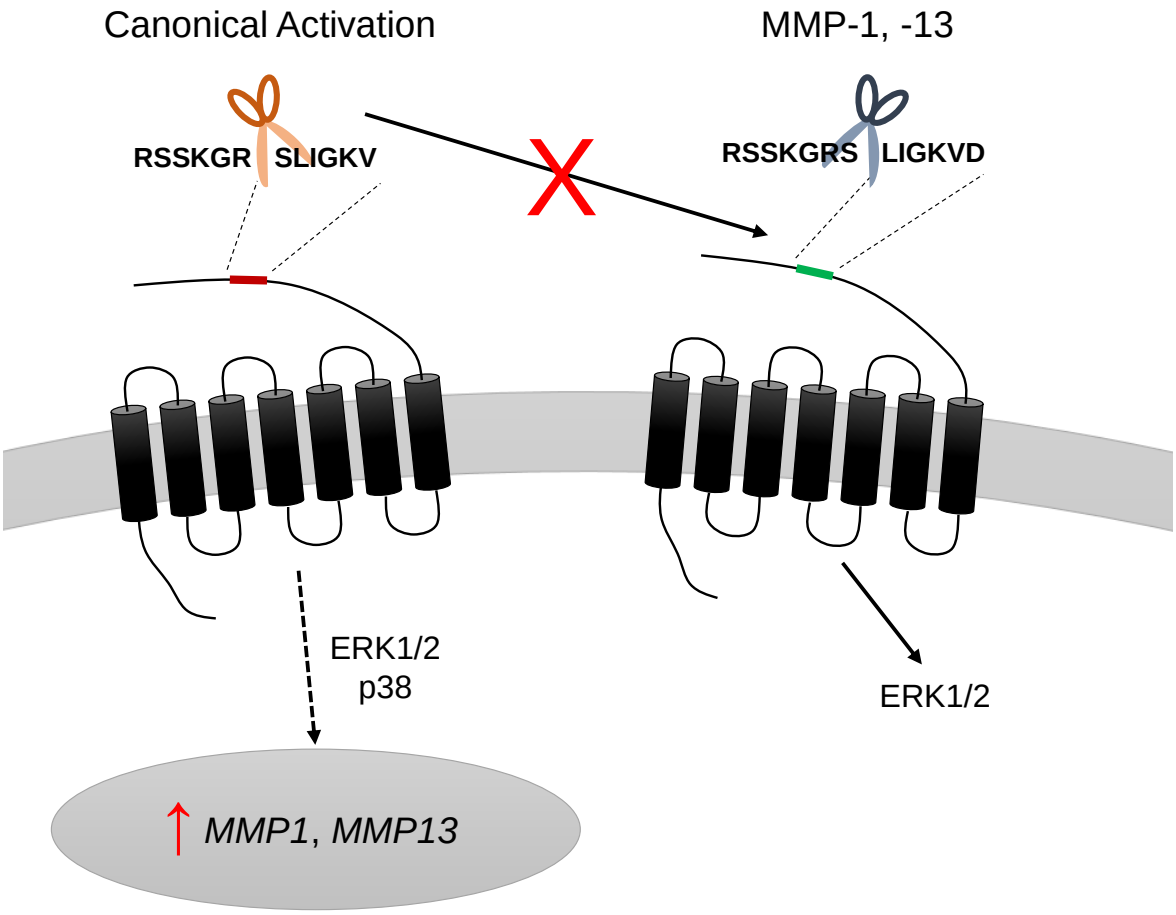

Figure 8: Collagenolytic MMPs are induced by PAR2 activation and can antagonise further PAR2 activation. Data presented within this study demonstrate that canonical PAR2 activation is able to induce *MMP1* and *MMP13* expression and subsequent secretion from chondrocytes, whilst the addition of MMP-1 to chondrocytes prior to canonical proteolytic stimulation results in an attenuated activation potential of PAR2.

Collagenolytic matrix metalloproteinases antagonise proteinase-activated receptor-2 activation, providing insights into extracellular matrix turnover

Adrian M.D. Falconer, Chun Ming Chan, Joseph Gray, Izuru Nagashima, Robert A. Holland, Hiroki Shimizu, Andrew R. Pickford, Andrew D. Rowan and David J. Wilkinson

J. Biol. Chem. published online May 19, 2019
